Solvation of Propylene Oxide in Water: Vibrational Circular Dichroism, Optical Rotation, and Computer Simulation Studies

Martin Losada, Phuong Nguyen, and Yunjie Xu*

Department of Chemistry, University of Alberta, Edmonton, Alberta, Canada T6G 2G2

Received: March 6, 2008; Revised Manuscript Received: April 8, 2008

The solvation of propylene oxide (PO) in water has been studied using vibrational circular dichroism (VCD) spectroscopy, optical rotation dispersion (ORD) spectroscopy, molecular dynamics simulations, and ab initio calculations. VCD and ORD measurements were carried out for PO as neat liquid, in CCl_4, and in water solutions. The classical molecular dynamics simulations were carried out for the PO + water binary mixtures at different concentrations, and the solvation information was derived from the radial distribution functions obtained in the simulations. The total number of water molecules within the closest vicinity of PO was predicted to be about 3. The geometry optimizations, vibrational frequencies, and VCD intensities were evaluated for the PO monomer and the PO−$(H_2O)_n$ clusters with $n = 1-3$, using density functional theory calculations at the B3LYP/aug-cc-pVTZ level of theory. The chirality transfer VCD feature, which is a direct result of the explicit H-bonding between water and the chiral PO solute, was detected experimentally at the water bending band region. This feature exhibits high sensitivity to the solvation structure around PO. Comparison of the calculated and experimental chirality transfer features leads to the conclusion that the PO−water binary complex is the dominating species in aqueous solution at room temperature and the anti conformation, where water is on the opposite side of the oxirane ring of the PO methyl group, is preferred over the syn one. This conclusion is also supported by the complementary ORD studies. Possible contributions from the ternary and quaternary PO−water complexes are also discussed.

Introduction

Water is the natural environment for many important biological processes. The hydration shell in the immediate vicinity of proteins, DNA, and other biological macromolecules often plays a major role in their stabilities and functions. For instance, the water molecules around hydrophobic and hydrophilic sites of enzyme proteins have been reported to participate directly in the molecular (chiral) recognition processes and can determine the outcome of the recognition processes.[1–3] It is therefore of great importance to understand the nature of the H-bonding interactions involving chiral molecules and water and the solvation of chiral molecules in aqueous solution. Vibrational circular dichroism (VCD) spectroscopy and optical rotation dispersion (ORD) spectroscopy have been documented to be highly sensitive to the solvent environments.[4] A long-standing problem in absolute structure determination using chiroptical measurements is how to account properly for such solvation effects. In recent years, there has been considerable progress in the theoretical modeling of chiroptical measurements and in the description of intermolecular interactions. We would like to take advantage of it to study the effects of water solvation on chiroptical measurements and in this process obtain direct information about the associated solvation structure in an aqueous environment.

Propylene oxide (PO) (Figure 1), a simple chiral building block, was chosen as our model system. PO has often served as a test case for the developments of VCD and OR theories because it is rigid except for its methyl group internal rotation and because it exists in one conformation.[5–7] Its structure was determined by rotational spectroscopy.[8,9] Its vibrational spectra as neat liquid and in solution were published in a number of studies,[10–12] and its VCD spectrum in the range of 850−1570 cm^{-1} [5,6,11,13] and its gas-phase[14,15] and solution-phase ORD spectra[15] were reported. Very recently, the rotational spectra of the PO−H_2O binary and the PO−$(H_2O)_2$ ternary complexes were reported, where both syn and anti conformers were detected experimentally.[16,17] While these experimental results represent an important step toward understanding the solvation structures and the intermolecular interactions taking place in an aqueous environment, there is still a lot of work to do to bridge the gap between the isolated PO−$(H_2O)_{1,2}$ systems and PO in water.

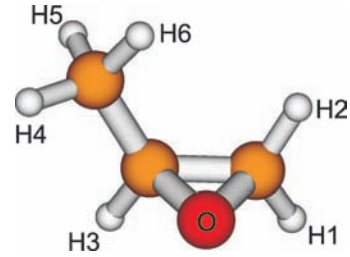

Figure 1. Optimized gas-phase structure of propylene oxide, computed at the B3LYP/aug-cc-pVTZ level of theory with atom labeling.

In this article, we present the VCD and ORD spectroscopic observations of PO as neat liquid, in CCl_4, and in water to unveil the effects of the explicit PO−water interactions on chiroptical measurements. We combined VCD and ORD spectroscopy with quantum chemistry ab initio calculations and classical molecular dynamics (MD) simulations to shed light on the hydration structure around PO in an aqueous environment. In particular, we show that the bending bands of the achiral water molecules can gain VCD strength through explicit hydrogen-bonding to

* Corresponding author. Telephone: 780-492-1244. Fax: 780-492-8231. E-mail: yunjie.xu@ualberta.ca.

10.1021/jp801996m CCC: $40.75
Published on Web 06/04/2008

the chiral PO solute. This chirality transfer VCD feature exhibits great sensitivity to the solvation structure around PO.

Experimental Methods

(*S*)- and (*R*)-PO, 99%, and racemic-PO, 99%, were obtained from Aldrich and used without any further purification. Both (*S*)- and (*R*)- and racemic-PO were dried using sodium sulfate. The residual water was monitored by taking VA spectra of the dried samples until no water absorptions were detected. The VA and VCD spectra in the range 850−1700 cm^{-1} were measured using a Bruker Vertex70 Fourier transform infrared spectrometer coupled to a PMA 50 VCD module.[18,19] A variable path length cell with BaF_2 windows and a low pass filter with a cutting wavenumber ~1800 cm^{-1} were used for the measurements. A spectral resolution of 4 cm^{-1} was used for all measurements. The VA and VCD spectra of the PO neat liquid were measured using a 15-μm path length and a data collection time of 1 h (3 × 20 min). Since PO is quite volatile, parafilm was used to prevent evaporation of PO. In addition, a new sample was used for every 20 min of measurement. For PO in the CCl_4 and H_2O solvents, the corresponding spectra were measured for (*S*)- and (*R*)-PO at 7 M using a path length of 15 μm and a 2-h data collection time (6 × 20 min). In the presented VA spectra, the solvent absorption was subtracted. All VCD measurements were performed for the enantiopure as well as for the racemic-PO samples. The presented VCD spectra were obtained by subtracting the racemic spectra from the enantiopure spectra. This was done to minimize any artifacts that are not due to chirality since VCD signals are typically 10^4-10^6 times weaker than the related VA signals. The OR experiments were measured at five discrete wavelengths (i.e., 365, 436, 546, 578, and 589 nm) using a commercial polarimeter (Perkin-Elmer 241; 1-dm sample path length). The OR measurements were obtained for PO neat liquid, for three concentrations of PO in CCl_4 at 0.0581, 0.2033, and 0.3602 g/mL, and for five concentrations of PO in water at 0.0581, 0.1162, 0.2033, 0.2905, and 0.3602 g/mL, corresponding roughly to 1, 2, 3.5, 5, and 7 M, respectively. All measurements and calculations are referred to as (*S*)-PO unless otherwise specified.

Computational Methods

Ab Initio. The geometry optimizations, harmonic frequency calculations, the VA and VCD intensity calculations, and the OR predictions were performed using the Gaussian03 suite of program packages.[20] The geometries of PO and the PO−$(H_2O)_n$ complexes with $n = 1, 2, 3$ were optimized using the Kohn−Sham density functional theory (DFT) with aug-cc-pVTZ basis set and the Becke three-parameter hybrid exchange-correlation functional known as B3LYP.[21] The functional and basis sets were chosen for their reliability in describing H-bonding interactions.[18,19] The geometries were fully optimized without symmetry restrictions, and the most stringent convergence criteria (e.g., gradient norm < 10^{-6} au) were used in all cases. The raw energies were corrected for the zero point energy (ZPE) effect and for the basis set superposition error (BSSE) using the full counterpoise procedure.[22,23] The reported DFT harmonic frequencies were uniformly scaled with a scaling factor of 0.988 to obtain best agreement between calculated and measured infrared frequencies empirically.[24] The OR calculations were carried out using time-dependent DFT methods and gauge-including atomic orbitals as implemented in Gaussian03.

Molecular Dynamics Simulations. All the MD simulations were carried out using the Sander module in the AMBER9 suite of programs.[25] The LEaP module of the AMBER9 package was used to build the starting configuration of PO. The structure was solvated in a truncated octahedral box with 406 pre-equilibrated TIP4P water molecules. TIP4P[26] was used because it shows good agreement with the experimental data for the structure of liquid water as TIP5P does,[27,28] and outperforms the three-site model (TIP3P) alternative.[29] The initial configuration was relaxed by applying 500 steps of steepest descent algorithm followed by 500 steps of conjugate gradient algorithm to remove bad contacts. The final configuration obtained was then used as the starting point for a 400-ps heating and equilibrating MD simulation under NVT conditions. The system was first heated from 0 to 300 K in 100 ps and was then equilibrated for 300 ps to ensure that the equilibrium was reached completely. A 6.9-ns production MD simulation was then performed under NPT conditions ($T = 300$ K, $P = 1$ atm). The particle mesh Ewald summation method[30,31] was used to treat the long-range electrostatic interactions, and the SHAKE algorithm[32] was used to constrain all covalent bonds involving the hydrogen atoms. A 6 Å cutoff was set for the nonbonded interactions. The MD simulation time step was 2 fs.

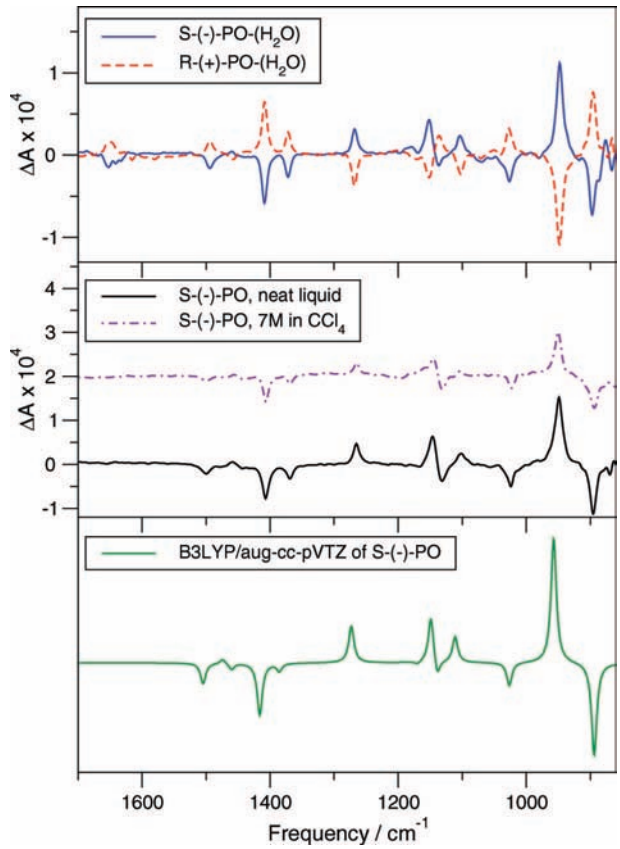

Figure 2. Experimental VCD spectra of PO in H_2O (top), as neat liquid, and in CCl_4 (middle) and the calculated VCD spectrum of PO (bottom).

Results and Discussion

Experimental Observation of Explicit Solute−Solvent H-Bonding Interactions in Water. The VCD spectra of PO neat liquid, PO in CCl_4, and PO in H_2O are shown in Figure 2. The VCD spectrum in the CCl_4 solution is very similar to that of PO neat liquid, with no additional new features. The gas-phase VCD calculation of the PO monomer at the B3LYP/aug-cc-pVTZ level of theory is also given in Figure 2. There is a very good agreement between the calculated and the experimentally observed spectra of neat liquid and of PO in CCl_4.

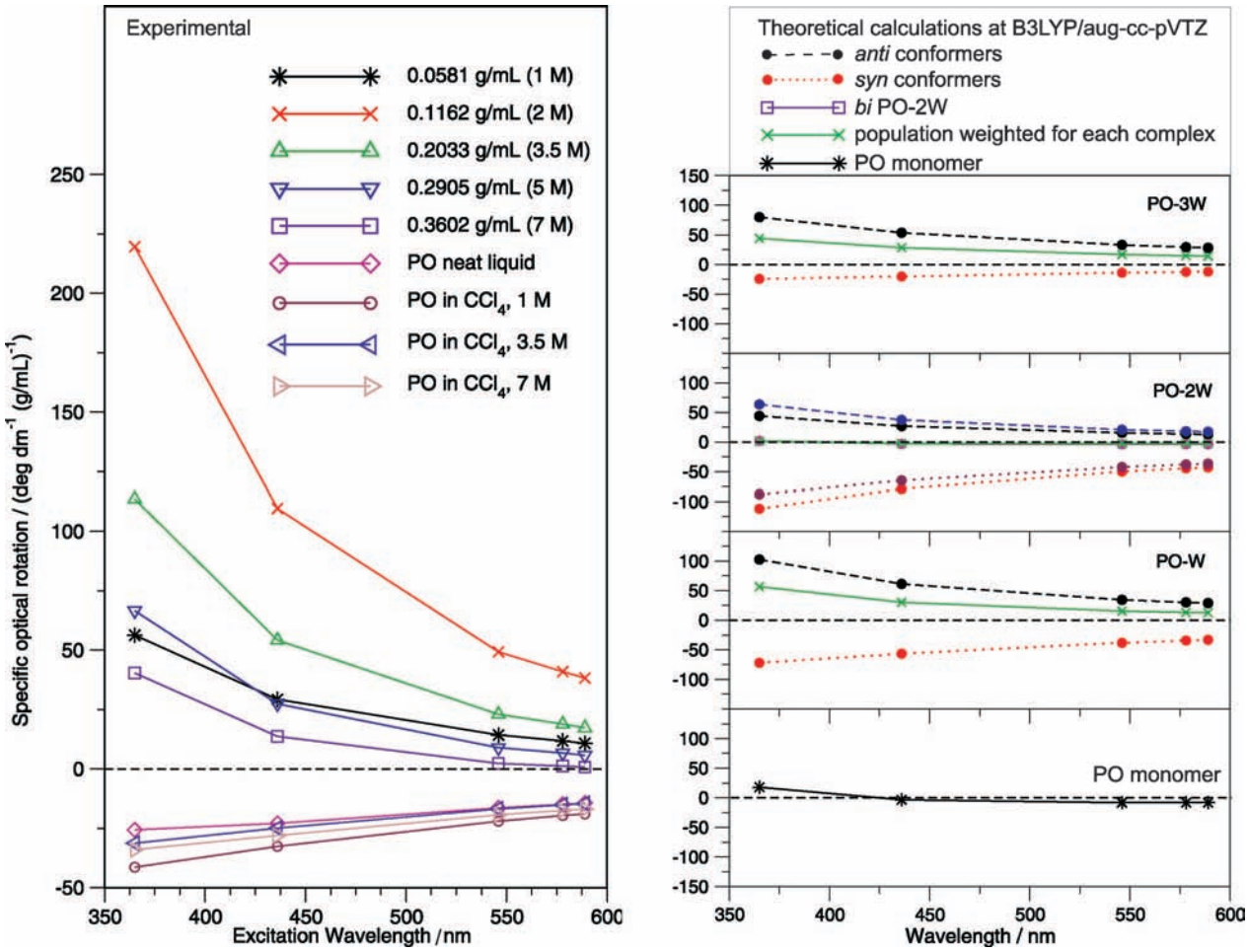

Figure 3. Left: Experimental ORD spectra of PO in water, in CCl_4, and as neat liquid. Right: Theoretical ORD spectra of the PO−$(H_2O)_{1,2,3}$ complexes and of the PO monomer computed at the B3LYP/aug-cc-pVTZ level. The dash traces are for the anti conformers and dotted traces for the syn conformers. For PO−2W, the traces from top to bottom are *anti*-PO−2W-I, *anti*-PO−2W-II, *bi*-PO−2W, *syn*-PO−2W-II, and *syn*-PO−2W-I. The predicted population weighted spectrum for each complex is presented by the solid cross trace.

This supports the conclusion that the PO−PO and PO−CCl_4 interactions are weak and nonspecific. As mentioned in the Introduction, the experimental VCD spectra of PO as neat liquid and in CCl_4 solution in the 850−1570 cm^{-1} region have been reported previously.[5,6,11,13] Our results in this frequency region are in good agreement with the earlier work. The experimental VCD spectrum of PO in water, on the other hand, shows a distinct new feature centered at 1650 cm^{-1} , the water bending band region. This feature has no counterpart in CCl_4 or in PO neat liquid. To be certain that this is not an artifact, parallel experiments were carried out for (*R*)-PO, and all bands observed, including the new band, show opposite signs (Figure 2), as expected. This new feature is attributed to the bending motions of the water subunits that are H-bonded to PO. The observation could be thought of as chirality transfer (i.e., some absorption bands of an achiral molecule such as H_2O become VCD active through explicit H-bonding with a chiral molecule such as PO). Similar phenomena were observed experimentally and theoretically before by our group and others.[18,19,33–35] This is direct experimental evidence of the effects of the explicit solvent−solute interactions on chiroptical measurements.

In a recent review, Polavarapu emphasized the importance of using more than one chiroptical spectroscopic method for the determination of the structures of chiral molecules.[36] To complement the above VCD investigation of the explicit intermolecular interactions in solution, we also carried out OR measurements for the three cases of PO discussed above. The ORD curves of PO neat liquid, PO in CCl_4, and PO in water at several different concentrations are plotted in the left panel of Figure 3. In general, the specific OR values of PO in CCl_4 show only small concentration dependence and are of similar magnitude and of the same sign as that of PO neat liquid. For comparison, the two gas phase specific OR values at 355 and 633 nm obtained by Vaccaro and co-workers[14,15] are 7.5 and −8.4 deg dm^{-1} $(g/mL)^{-1}$, respectively. The specific OR values of PO in water, however, exhibit strong concentration dependence with large magnitude fluctuation and are of the opposite sign to that of PO neat liquid and of PO in CCl_4. The specific OR value of PO in water increases going from 0.0581 (1 M) to 0.1162 g/mL (2 M) reaches a maximum value at 2 M, then decreases as the concentration increases to 0.3602 g/mL (7 M) where the solution is saturated. This trend is true for all five experimental wavelengths used. This significant difference observed with different solvents can be attributed to the weak nonspecific interactions in PO neat liquid and in the PO CCl_4 solution and the explicit solvent−solute H-bonding interactions in the PO H_2O solution (vide infra). The gas-phase OR measurements of PO and the effects of nonspecific solute−solvent interactions on them have been the subjects of intensive experimental and theoretical interest in recent years.[7,15,37] In this article, we will mainly focus on the explicit solute−solvent intermolecular interactions.

Theoretical Interpretations. To explain the above observation and to further understand the solution structure, molecular

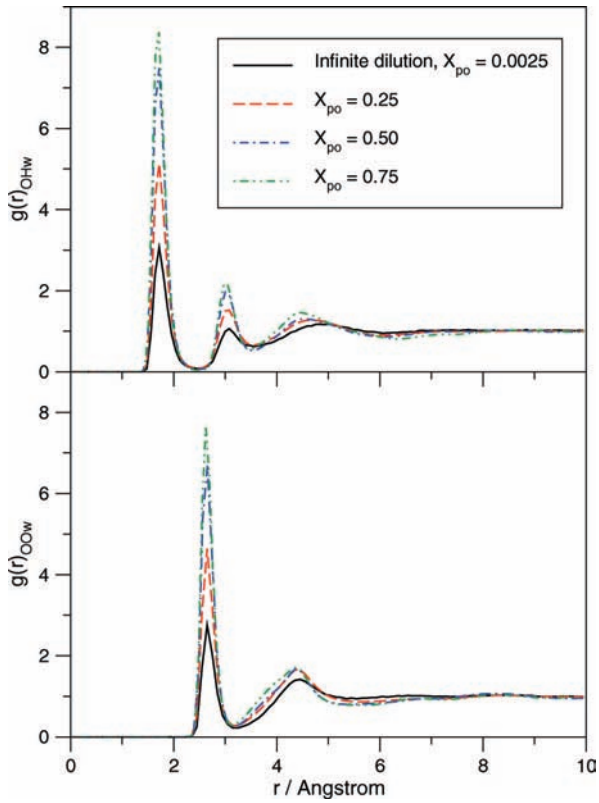

Figure 4. Site−site radial distribution functions for the PO + H_2O binary mixtures with different PO molar fractions. Ow and Hw are water oxygen and water hydrogen, respectively.

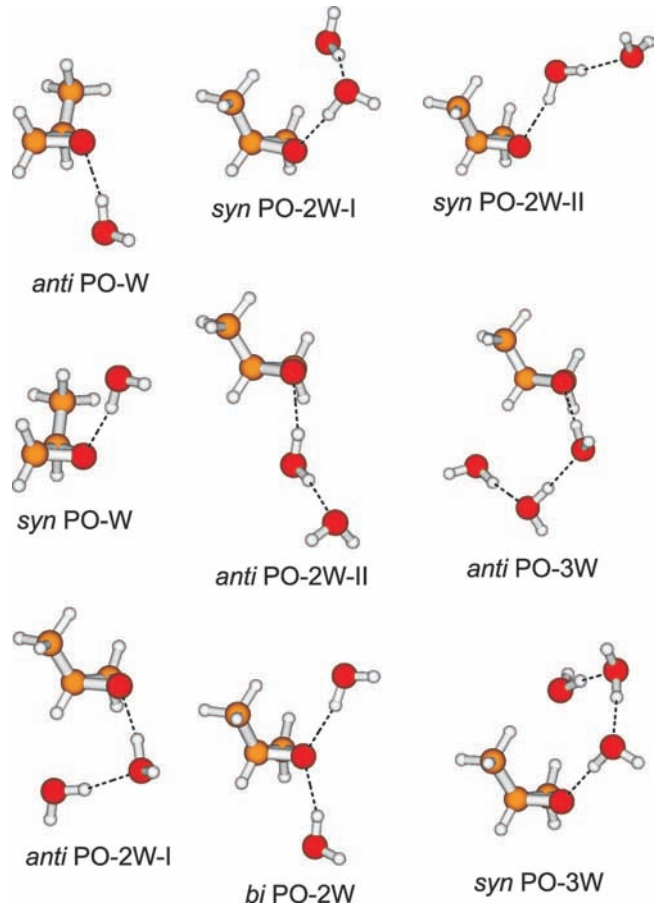

Figure 5. Optimized geometries of the PO−$(H_2O)_{1,2,3}$ conformers at the B3LYP/aug-cc-pVTZ level of theory.

dynamics (MD) simulations were used to describe the solvent environment surrounding PO. MD simulations for the PO + H_2O binary mixtures were carried out for 0.0025, 0.25, 0.50, and 0.75 PO mole fractions. The first one corresponds to a highly diluted situation where the PO−PO interactions are minimized, while the others correspond to mole ratios of PO/H_2O of 1:3, 1:1, and 3:1. From the MD simulations, the site−site radial distribution functions (RDFs) of the H atoms and of the oxygen atom of the water molecules around the PO oxygen atom, denoted as $g(r)_{OHw}$ and $g(r)_{OOw}$, respectively, are presented in Figure 4. The first maximum in the RDFs $g(r)_{OHw}$ and $g(r)_{OOw}$ appear at 1.70 and 2.62 Å, respectively. The maximum at 1.7 Å describes the first shell of hydrogen atoms of water molecules around PO. The H-bonding nature of these interactions is clearly indicated by the very well defined peaks of both $g(r)_{OHw}$ and $g(r)_{OOw}$ functions. The observation is in line with the fact that the primary intermolecular interaction between PO and water is the H-bonding from the PO's oxygen atom to the H atom of water. Both RDFs show a second well-defined peak, suggesting that a second solvation shell is developed around the PO molecules. A detailed analysis of the $g(r)_{OHw}$ RDF at longer distances reveals a third shell. As the PO concentration increases, the intensities of the first and second maxima in $g(r)_{OHw}$ and $g(r)_{OOw}$ increase noticeably, while the peak positions remain the same. This indicates that the water molecules surrounding PO become more strongly correlated with each other, with increasing PO concentration. These observations lead to the conclusion that, when PO and water are mixed, H-bonding networks of the PO−$(H_2O)_n$ complexes are reinforced, giving rise to the heteroassociations where water is highly structured around PO.

The nature of the solute−solvent interactions is analyzed by studying the energetic and conformational properties of several complexes established by the heteroassociations between PO and water molecules. To analyze the solvation of PO by water molecules, explicit H-bonding interactions were considered by building the PO−$(H_2O)_n$ complexes. The number of water molecules (n) required to build the complexes is gathered from the above MD simulations. Integration of the first peak of the $g(r)_{OOw}$ RDF up to the first minimum at 3.15 Å results in a coordination number of 2.6. This value is in good agreement with the coordination number from the previous MD simulations reported by Beratan and co-workers[38] using the OPLS-AA force

TABLE 1: Counterpoised-Corrected (D_e^{BSSE}) Binding and ZPE (D_0^{BSSE})-Corrected Dissociation Energies (in kcal/mol), Relative Free Energies, and Populations of the Most Stable Complexes of PO−$(H_2O)_n$, with n = 1, 2, 3 at the B3LYP/aug-cc-pVTZ Level of Theory

conformer	D_e^{BSSE}	D_0^{BSSE}	ΔD_0^{BSSE}	ΔG	P (%)[a]
n = 1					
anti-PO−W	−5.0871	−3.3638	0	0	73.7
syn-PO−W	−4.9812	−3.1785	0.1853	0.6100	26.3
n = 2					
anti-PO−2W-I	−12.3671	−8.3110	0	0	58.5
syn-PO−2W-I	−12.2965	−8.1811	0.1300	0.6130	20.8
bi-PO−2W	−9.3336	−5.9429	2.3681	1.1439	8.5
anti-PO−2W-II	−8.4124	−5.0335	3.2775	1.3177	6.3
syn-PO−2W-II	−8.3067	−4.9564	3.3546	1.3491	5.9
n = 3					
anti-PO−3W	−20.2758	−14.0253	0	0	65.7
syn-PO−3W	−20.2771	−13.9255	0.0998	0.3852	34.3

[a] Populations based on ΔG values, T = 298 K.

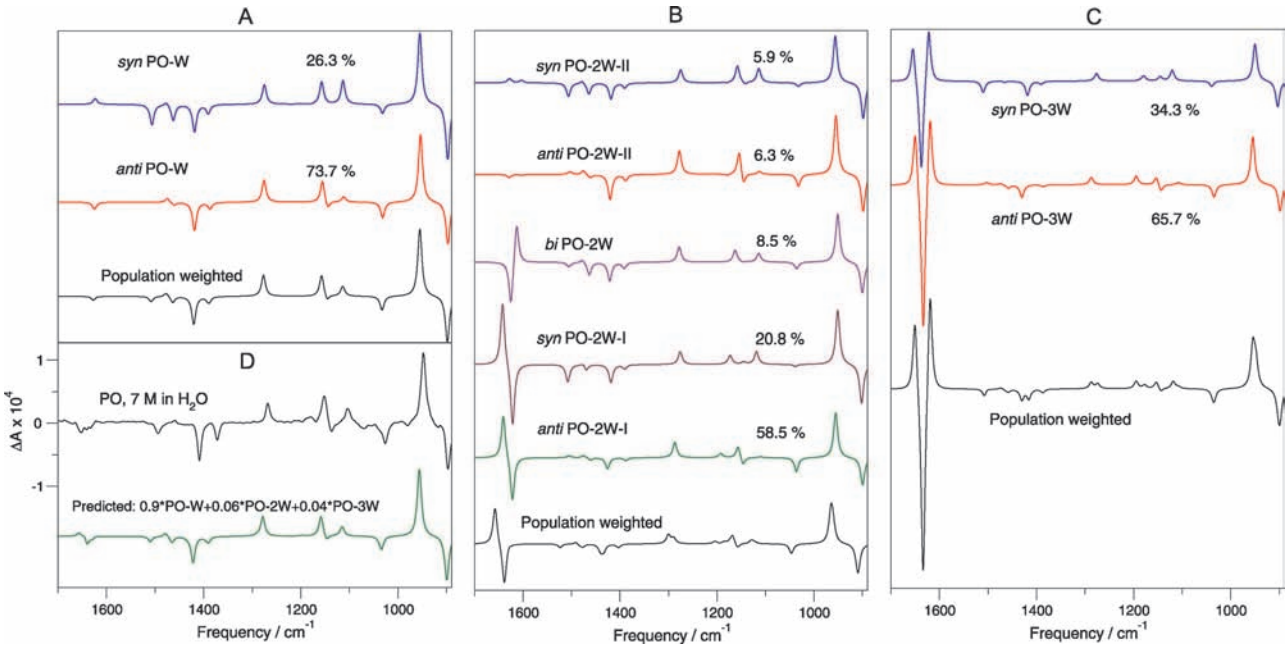

Figure 6. (A−C) Calculated VCD spectra of the PO−$(H_2O)_{1,2,3}$ conformers at the B3LYP/aug-cc-pVTZ level of theory, together with the population-weighted VCD spectra for each PO−water complex. (D) Experimental VCD spectrum for PO in water and the empirically weighted VCD spectrum based on the PO−$(H_2O)_{1,2,3}$ complexes.

field[39] and the SPC water model.[40,41] We will therefore use the PO−$(H_2O)_n$ complexes with $n = 1, 2, 3$ to model the explicit solute−solvent interactions in the PO water solution.

On the basis of the previous high-resolution spectroscopic and theoretical results,[16,17] we expect the PO−$(H_2O)_n$ complexes to form hydrogen bonds with the possibility for the water molecule(s) to lie on either side of the oxirane ring when interacting with the PO oxygen lone electron pairs. We use anti or syn to denote that the water molecule(s) is on the opposite or the same side of the PO methyl group, respectively, and use bi if the water molecules are on both sides of the oxirane ring, following the notation used in refs[16] and.[17] The B3LYP/aug-cc-pVTZ optimized geometries of the PO−$(H_2O)_{1,2,3}$ complexes are shown in Figure 5. Altogether, nine low-energy conformers were identified with two, five, and two conformers for the binary, ternary, and quaternary complexes, respectively. The raw and the ZPE- and BSSE-corrected dissociation energies of the conformers, as well as the corresponding Gibbs free energies at 298 K, were collected in Table 1, together with the predicted populations based on the relative Gibbs free-energy ΔG values. A few much higher energy conformers were also identified for the quaternary complex but are not included since they have no appreciable population at room temperature. The two PO−H_2O and the three lowest-energy PO−$(H_2O)_2$ conformers identified are consistent with those reported previously.[16,17]

To compare the experimental and calculated VCD spectra, we carried out vibrational frequency, absorption intensity, and VCD intensity calculations. The calculated VCD spectra of the binary, ternary, and quaternary PO−$(H_2O)_n$ conformers are displayed in Figure 6A−C, respectively, together with the corresponding population-weighted VCD spectra. While the VCD spectra corresponding to the PO subunit exhibit only minor changes among all conformers, the VCD signatures centered at the water bending bands (i.e., the chirality transfer spectral window) are dramatically different going from one conformer to the next. This observation highlights the great potential of utilizing the chirality transfer spectral window as a conformational marker to probe the explicit solute−solvent interactions in solution. For the binary complex, the VCD signal at the water bending band region is negative for *anti*-PO−H_2O and positive for *syn*-PO−H_2O. Of the ternary complex, the two dominant conformers (i.e., *syn*- and *anti*-PO−2W-I) show a strong bisignate VCD signal at the water bending region. The two quaternary conformers show an overwhelmingly intensive trisignate VCD signal in this chirality transfer spectral window. These signature features associated with the ternary and quaternary conformers are not visible in the experimental VCD spectrum. Inspection of the predicted and experimental VCD features in this spectral window leads to the conclusion that anti PO−H_2O is the dominant species in solution and the larger PO hydration clusters make little contribution to the observed VCD spectrum in water. This conclusion can be reached even without the detailed energetic values since the VCD signatures in this chirality transfer window are very distinctive for different conformers. It is also interesting to note that, while the relative dissociation energy predicts only a small preference for the *anti*-PO−H_2O over *syn*-PO−H_2O, the use of the relative Gibbs free energy leads to much larger preference for anti conformer and therefore better agreement with the experimental result. The importance of using ΔG rather then ΔD_0 for systems under equilibrium condition was discussed in other recent studies.[42] An empirically weighted VCD spectrum, including contributions from all the conformers considered in this study, is given in Figure 6D. The factors used are 0.90 for PO−W, 0.06 for PO−2W, and 0.04 for PO−3W to best reproduce the observed spectrum.

To interpret the complementary OR data, the specific OR values at the five experimental wavelengths were calculated using DFT at the B3LYP/aug-cc-pVTZ level for the PO−$(H_2O)_{1,2,3}$ clusters and the PO monomer. The calculated ORD curves are summarized in the right panel of Figure 3. The population weighted ORD curves for the PO−$(H_2O)_{1,2,3}$ complexes are also shown in Figure 3. The calculated specific OR values for the PO monomer are quite small and are negative at 436, 546, 578, and 589 nm, and positive at 365 nm. The trend predicted is in good agreement with the two gas-phase values

at 355 and 633 nm reported previously.[14,15] A few theoretical groups have pointed out that the apparent success of DFT in catching the correct signs of the gas phase specific OR values may be fortuitous, and the readers are referred to the recent review by Crawford and co-workers[7] for further details. The calculated values agree reasonably with the observed OR values for PO neat liquid and PO in CCl_4 at the four longer wavelengths. On the other hand, the experimental OR values for PO neat liquid and PO in CCl_4 become more negative at the shorter wavelengths, whereas the opposite was predicted for the PO monomer. Therefore, the PO−PO and PO−CCl_4 interactions play a role here. But the effects due to the PO−water explicit H-bonding interactions are much more severe. The calculated specific OR values for the anti conformers of the binary, ternary, and quaternary PO−water complexes are all positive, while those of the syn conformers are all negative. The *bi*-PO−2W conformer exhibits essentially zero OR. Comparing the predicted and the experimental ORD curves, one may conclude that there is a preference for the anti over the syn conformers. A similar conclusion was drawn in the previous MD simulation study.[38] As mentioned before in the VCD discussion, the predicted relative Gibbs free energies indeed show a preference for the anti over syn conformers. For the PO−$(H_2O)_2$ ternary complex, the population weighted specific OR values from the five conformers are close to zero at all five wavelengths measured. Therefore, the ternary PO−water complex does not contribute much to the observed ORD curves. The population-weighted ORD curves of the binary PO−H_2O and the quaternary PO−$(H_2O)_3$ complexes are quite similar and are of the same sign as the experimental ORD curves. For the 7 M solution at which the VCD experiment was performed, the population-weighted ORD curve of the binary PO−H_2O is in good agreement with the experimental curve. This is in accord with the conclusion derived from the VCD study that the binary PO−H_2O is the dominant species in water, although the OR data alone can not differentiate the contributions by the binary or quaternary complexes. An interesting feature observed experimentally is that the specific OR value maximized at the concentration of 2 M. The exact cause is difficult to pin down on the basis of the current OR calculations, in particular, since a quantitative agreement between the experiment and theory for even the gas-phase PO monomer is yet to be achieved.[7] It would be helpful to perform VCD measurements at these more diluted concentrations to detect any noticeable changes in the chirality transfer spectral window. Unfortunately, several attempts on this were not successful because of technical challenges. The water bending band is a very intense vibrational absorption band, and therefore an extremely thin path length is needed to ensure a proper subtraction for VCD measurements. This further reduces the number of PO molecules available for detection, making it extremely difficult if not impossible to obtain a reliable VCD spectrum in this spectral window.

Conclusions

The effects of explicit solute−solvent H-bonding on the VCD and OR measurements of PO in water were investigated using chiroptical spectroscopy, DFT calculations, and MD simulations. The analysis of the MD simulations indicates that a solvation structure is developed around PO molecules in the PO + water binary mixtures, giving rise to the reinforced H-bonding networks as suggested by the well-defined maxima for both $g(r)_{OHw}$ and $g(r)_{OOw}$. Further DFT calculations show that the experimentally observed effects can be adequately explained by considering the PO−water clusters. In particular, the VCD signatures in the chirality transfer spectral window lead to the conclusion that the binary PO−H_2O complex is the dominating species in aqueous solution at room temperature and that the anti conformation is preferred over the syn one. This conclusion is supported by the complementary OR investigation. This work also illustrates the power of VCD spectroscopy, in combination with theoretical modeling and OR spectroscopy, to probe the solvation structure of a chiral molecule in aqueous environments.

Acknowledgment. This research was funded by the University of Alberta, the Natural Sciences and Engineering Research Council of Canada, the Canada Foundation for Innovation (New Opportunity), Alberta Ingenuity (New Faculty Award and New Faculty Extension Award), and Petro-Canada (Young Innovator Award). We thank W. Moffat for the optical rotation measurements and Drs. P. N. Roy and G. Yang for discussions. We also gratefully acknowledge access to the computing facilities provided by the Academic Information and Communication Technology group at the University of Alberta.

References and Notes

(1) Svergun, D. I.; Richard, S.; Koch, M. H. J.; Sayers, Z.; Kuprin, S.; Zaccia, G. *Proc. Natl. Acad. Sci. U.S.A.* **1998**, *95*, 2267.
(2) Makarov, V. A.; Feig, M.; Andrews, B. K.; Pettit, B. M. *Biophys. J.* **1998**, *75*, 150.
(3) Pal, S. K.; Peon, J.; Zewail, A. H. *Proc. Natl. Acad. Sci. U.S.A.* **2002**, *99*, 1763.
(4) Eliel, E. L.; Wilen, S.; Doyle, M. P. *Basic Organic Stereochemistry*; Wiley-Interscience: New York, 2001.
(5) Kawiecki, R. W.; Devlin, F.; Stephens, P. J.; Amos, R. D.; Handy, N. C. *Chem. Phys. Lett.* **1988**, *145*, 411.
(6) Kawiecki, R. W.; Devlin, F.; Stephens, P. J.; Amos, R. D. *J. Phys. Chem.* **1991**, *95*, 9817.
(7) Crawford, T. D.; Tam, M. C.; Abrams, M. L. *J. Phys. Chem. A* **2007**, *111*, 12057.
(8) Creswell, R. A.; Schwendeman, R. H. *J. Mol. Spectrosc.* **1977**, *64*, 295.
(9) Imachi, M.; Kuczkowski, R. L. *J. Mol. Struct.* **1982**, *96*, 55.
(10) Villareal, J. R.; Laane, J. *J. Chem. Phys.* **1975**, *62*, 303.
(11) Polavarapu, P. L.; Hess, B. A., Jr.; Schaad, L. J. *J. Chem. Phys.* **1985**, *82*, 1705.
(12) Lowe, M. A.; Alper, J. S.; Kawiecki, R.; Stephens, P. J. *J. Phys. Chem.* **1986**, *90*, 41.
(13) Polavarapu, P. L.; Michalska, D. F. *J. Am. Chem. Soc.* **1983**, *105*, 6190.
(14) Müller, T.; Wiberg, K. B.; Vaccaro, P. H. *J. Phys. Chem. A* **2000**, *104*, 5959.
(15) Wilson, S. M.; Wiberg, K. B.; Cheeseman, J. R.; Frisch, M. J.; Vaccaro, P. H. *J. Phys. Chem. A* **2005**, *109*, 11752.
(16) Su, Z.; Wen, Q.; Xu, Y. J. *J. Am. Chem. Soc.* **2006**, *128*, 6755.
(17) Zheng, S.; Xu, Y. J. *Angew. Chem.* **2007**, *119*, 6275; *Angew. Chem., Int. Ed.* **2007**, *46*, 6163.
(18) Losada, M.; Xu, Y. J. *Phys. Chem. Chem. Phys.* **2007**, *9*, 3127.
(19) Losada, M.; Tran, H.; Xu, Y. J. *J. Chem. Phys.* **2008**, *128*, 014508.
(20) Frisch, M. J.; Trucks, G. W.; Schlegel, H. B.; Scuseria, G. E.; Robb, M. A.; Cheeseman, J. R.; Montgomery, J. A., Jr.; Vreven, T.; Kudin, K. N.; Burant, J. C.; Millam, M.; Iyengar, S. S.; Tomasi, J.; Barone, V.; Mennucci, V.; Cossi, M.; Scalmani, G.; Rega, N.; Petersson, G. A.; Nakatsuji, H.; Hada, M.; Ehara, M.; Toyota, K.; Fukuda, R.; Hasegawa, J.; Ishida, M.; Nakajima, T.; Honda, Y.; Kitao, O.; Nakai, H.; Klene, M.; Li, X.; Knox, J. E.; Hratchian, H. P.; Cross, J. B.; Adamo, C.; Jaramillo, J.; Gomperts, R.; Stratmann, R. E.; Yazyev, O.; Austin, A. J.; Cammi, R.; Pomelli, C.; Ochterski, J. W.; Ayala, P. Y.; Morokuma, K.; Voth, G. A.; Salvador, P.; Dannenberg, J. J.; Zakrzewski, V. G.; Dapprich, S.; Daniels, A. D.; Strain, M. C.; Farkas, O.; Malick, D. K.; Rabuck, A. D.; Raghavachari, K.; Foresman, J. B.; Ortiz, J. V.; Cui, Q.; Baboul, A. G.; Clifford, S.; Cioslowski, J.; Stefanov, B. B.; Liu, G.; Liashenko, A.; Piskorz, P.; Komaromi, I.; Martin, R. L.; Fox, D. J.; Keith, T.; Al-Laham, M. A.; Peng, C. Y.; Nanayakkara, A.; Challacombe, M.; Gill, P. M. W.; Johnson, B.; Chen, W.; Wong, M. W.; Gonzalez, C.; Pople, J. A. *Gaussian 03*, revision B.05; Gaussian, Inc.: Pittsburgh, PA, 2003.
(21) (a) Becke, A. D. *J. Chem. Phys.* **1993**, *98*, 1372. (b) Becke, A. D. *J. Chem. Phys.* **1993**, *98*, 5648. (c) Lee, C. T.; Yang, W. T.; Parr, R. G. *Phys. Rev. B* **1988**, *37*, 785.
(22) Boys, S. F.; Bernardi, F. *Mol. Phys.* **1970**, *19*, 553.
(23) Xantheas, S. S. *J. Chem. Phys.* **1996**, *104*, 8821.

(24) Merrick, J. P.; Moran, D.; Radom, L. *J. Chem. Phys. A* **2007**, *111*, 11683.
(25) Case, D.A.; Darden, T.A.; Cheatham, T.E., III; Simmerling, C. L.; Wang, J.; Duke, R. E.; Luo, R.; Merz, K. M.; Pearlman, D. A.; Crowley, M.; Walker, R. C.; Zhang, W.; Wang, B.; Hayik, S.; Roitberg, A.; Seabra, G.; Wong, K. F.; Paesani, F.; Wu, X.; Brozell, S.; Tsui, V.; Gohlke, H.; Yang, L.; Tan, C.; Mongan, J.; Hornak, V.; Cui, G.; Beroza, P.; Mathews, D. H.; Schafmeister, C.; Ross, W. S.; Kollman, P. A. *AMBER 9*; University of California, San Francisco, CA, 2006.
(26) Jorgensen, W. L.; Chandrasekhar, J.; Madura, J. D.; Impey, R. W.; Klein, M. L. *J. Chem. Phys.* **1983**, *79*, 926.
(27) Mahoney, M. W.; Jorgensen, W. L. *J. Chem. Phys.* **2000**, *112*, 8910.
(28) Mantz, Y. A.; Chen, B.; Martyna, G. J. *J. Phys. Chem. B* **2006**, *110*, 3540.
(29) Jorgensen, W. L.; Jenson, C. *J. Comput. Chem.* **1998**, *19*, 1179.
(30) Ding, H. Q.; Karasawa, N.; Goddard, W. A. *J. Chem. Phys.* **1992**, *97*, 4309.
(31) Essmann, U.; Perera, L.; Berkowitz, M. L.; Darden, T.; Lee, H.; Pedersen, L. G. *J. Chem. Phys.* **1995**, *103*, 8577.
(32) Ryckaert, J. P.; Ciccotti, G.; Berendsen, H. J. C. *J. Comput. Phys.* **1977**, *23*, 237.
(33) Sadlej, J.; Dobrowolski, J. C.; Rode, J. E.; Jamróz, M. H. *Phys. Chem. Chem. Phys.* **2006**, *8*, 101.
(34) Bürgi, T.; Vargas, A.; Baiker, A. *J. Chem. Soc., Perkin Trans.* **2002**, *2*, 1596.
(35) Allenmark, S. *Chirality* **2003**, *15*, 409.
(36) Polavarapu, P. L. *Chirality* **2008**, *20*, 664.
(37) Fischer, A. T.; Compton, R. N.; Pagni, R. *J. Phys. Chem. A* **2006**, *110*, 7067.
(38) Mukhopadhyay, G.; Zuber, G.; Goldsmith, M.-R.; Wipf, P.; Beratan, D. N. *ChemPhysChem* **2006**, *7*, 2483.
(39) Jorgensen, W. L.; Maxwell, D. S.; Tirado-Rives, J. *J. Am. Chem. Soc.* **1996**, *118*, 11225.
(40) Berendsen, H. J.; Postma, J. P.; van Gunsteren, W. F.; Hermans, J. In *Intermolecular Forces*; Pullman, B., Ed.; D. Reidel: Dordrecht, The Netherlands, 1981; p 331.
(41) Berweger, C. D.; van Gunsteren, W. F.; Müller-Plathe, F. *Chem. Phys. Lett.* **1995**, *232*, 429.
(42) Wilson, S. M.; Wiberg, K. B.; Murphy, M. J.; Vaccaro, P. H. *Chirality* **2008**, *20*, 357.

JP801996M